processes

MDPI

Article

Supported Ionic Liquid Membranes for Separation of Lignin Aqueous Solutions

Ricardo Abejón *, Javier Rabadán, Silvia Lanza, Azucena Abejón, Aurora Garea and Angel Irabien

Chemical and Biomolecular Engineering Department, University of Cantabria. Avda. Los Castros s/n, 39005 Santander, Spain; javier.rabadan.mtz@gmail.com (J.R.); silvialan19@gmail.com (S.L.); azucena.abejon@unican.es (A.A.); aurora.garea@unican.es (A.G.); angel.irabien@unican.es (A.I.)

* Correspondence: abejonr@unican.es; Tel.: +34-9-4220-1579; Fax: +34-9-4220-1591

Received: 3 August 2018; Accepted: 28 August 2018; Published: 1 September 2018

Abstract: Lignin valorization is a key aspect to design sustainable management systems for lignocellulosic biomass. The successful implementation of bio-refineries requires high value added applications for the chemicals derived from lignin. Without effective separation processes, the achievement of this purpose is difficult. Supported ionic liquid membranes can play a relevant role in the separation and purification of lignocellulosic components. This work investigated different supported ionic liquid membranes for selective transport of two different types of technical lignins (Kraft lignin and lignosulphonate) and monosaccharides (xylose and glucose) in aqueous solution. Although five different membrane supports and nine ionic liquids were tested, only the system composed by [BMIM][DBP] as an ionic liquid and polytetrafluoroethylene (PTFE) as a membrane support allowed the selective transport of the tested solutes. The results obtained with this selective membrane demonstrated that lignins were more slowly transferred from the feed compartment to the stripping compartment through the membrane than the monosaccharides. A model was proposed to calculate the effective mass transfer constants of the solutes through the membrane (values in the range 0.5–2.0 $\times$ 10^{-3} m/h). Nevertheless, the stability of this identified selective membrane and its potential to be implemented in effective separation processes must be further analyzed.

Keywords: supported ionic liquid membranes; separation; lignin; glucose; xylose

1. Introduction

Among renewable raw materials, wood must be highlighted, because more effective, cost-competitive and sustainable alternatives have not been identified for some applications. Forest exploitation provides economic and social values from this natural resource and promotes a sustainable development chance for rural areas [1]. The wood processing industrial sector obtains forest products such as lumber, engineered wood, and pulp. Traditional wood pulping has been focused on the fractionation of the main lignocellulosic components (cellulose, hemicellulose, and lignin), but paying special attention to the cellulosic fraction, which is the relevant one for the production of paper. In this framework, hemicellulose and lignin have been only employed for energy recovery by direct combustion [2]. However, recent research interest is being targeted to hemicellulose and lignin as raw materials for renewable chemicals to replace those derived from petroleum. Therefore, the integral use of the lignocellulosic biomass must take into account the valorization of hemicellulose and lignin [3–5]. For example, lignin must be considered the most promising renewable source to produce aromatic chemicals at a real industrial scale because of its structure (Figure 1) and its abundance in nature [6].

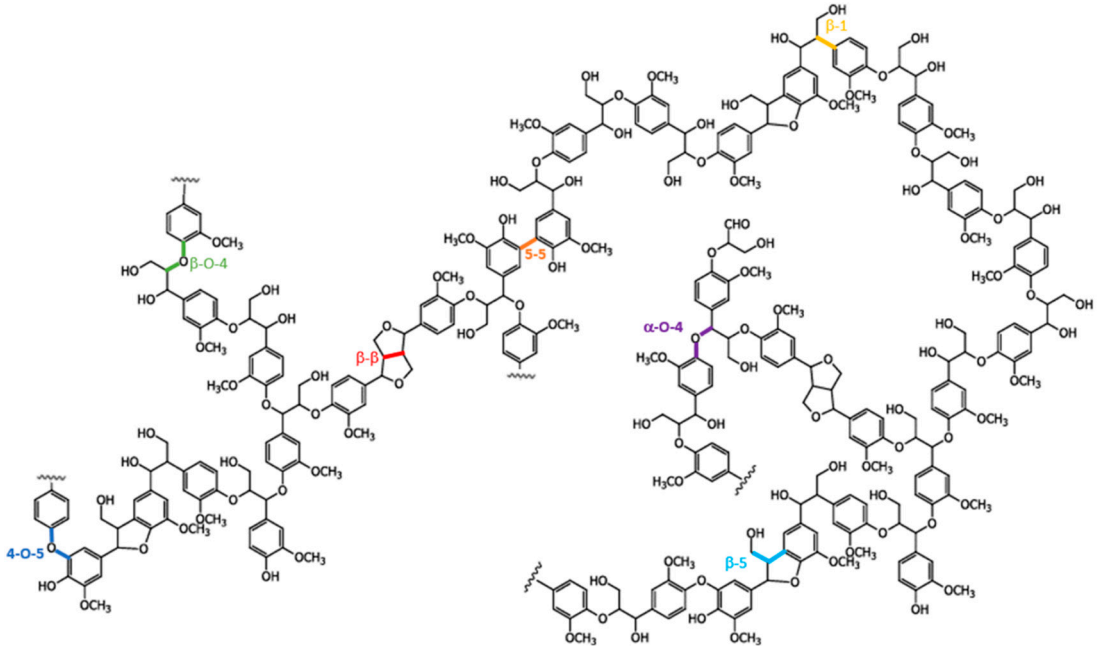

Figure 1. Example of lignin structure. Reproduced with permission from Chávez-Sifontes, Lignina, estructura y aplicaciones: métodos de despolimerización para la obtención de derivados aromáticos de interés industrial; published by Avances en Ciencias e Ingeniería, 2013.

In this new scenario, biorefineries have been introduced to provide an alternative to traditional petroleum refineries. A biorefinery is a facility that integrates the biomass conversion processes to produce bioenergy, biofuels, and bio-based chemicals from biomass [7]. While the valorization of cellulose and hemicellulose has been successfully implemented in biorefineries [8], the optimal valorization of lignin remains as a great challenge to be solved. Enzymatic hydrolysis of cellulose and hemicellulose results in fermentable sugars, which can be easily transformed to biofuels (bioethanol) or precursors for production of valuable bio-based chemicals. Delignification is a necessary prerequisite for enzymatic hydrolysis, as lignin interferes the reaction and blocks the process [9,10]. Therefore, lignin must be separated during the pretreatment of lignocellulosic biomass, which facilitates its posterior valorization.

The production of commercially available lignin-derived chemicals has been very limited until recent days: only dispersing and emulsifying agents obtained from lignosulphonates and plywood panels can be mentioned. This lack of commercial application can be justified by the heterogeneous structure of lignin, which, unlike cellulose or hemicellulose, is not formed by the systematic series of regular monomers. Despite this irregular and complex structure, research efforts have been applied to find the most suitable options for lignin conversion to valuable products [11–16]. Although some possibilities have been identified for direct valorization of raw lignin, lignin depolymerization is a more promising route. On the one hand, aggressive unselective depolymerization to break C-C and C-O linkages results in aromatic compounds mixtures like benzene, toluene, xylene, and phenol [17,18]. In addition, some short aliphatic (C1-C3) and, in less extent, longer cycloaliphatic (C6-C7) hydrocarbons can be obtained. On the other hand, highly selective depolymerization processes are based on the cleavage of only determined links. This way, products that are not easily produced by traditional petrochemical routes can be obtained, like substituted coniferols, aromatic polyols, or oxidized monomers [19].

However, classic fractionation processes for lignocellulosic biomass (Kraft process, Organosolv process, alkaline treatment, steam explosion ...) result in low-purity lignin, mostly because of the presence of impurities derived from cellulose and hemicellulose. Consequently, new research efforts

must be applied to develop an efficient and selective process to obtain a purified lignin fraction. Membrane separation technologies have been implemented in biorefineries because they show very advantageous properties: no phase change, no heat requirements, low energy consumption, and compact and easily scalable design [20]. Research works have investigated the potentiality of membrane techniques for lignin separation and purification. Lignin-rich liquors can be treated with ultrafiltration and nanofiltration membranes for purification of lignin and separation of other inorganic compounds [21–26]. Other authors have applied membrane separations for different tasks aimed to lignin valorization, such as concentration of lignin solutions and elimination of lower molecular weight impurities [27], fractionation of lignin fragments according to their molecular weight [28,29], or separation of different lignin derivatives [30–32].

Since lignin is not easily solubilized in conventional solvents, the use of ionic liquids (ILs) for fractionation of lignocellulosic biomass has been deeply investigated. ILs are organic salts formed by high-volume organic cations and smaller organic or inorganic anions. Some of the most interesting ILs have melting points below 100 °C, so they are liquid at room temperature. These ILs present some common characteristics, like negligible vapor pressure or high thermal and mechanic stabilities [33]. The physicochemical properties can be customized by an optimal combination of the most convenient cations and anions for each application. The viability of ILs for dissolution, separation, and recovery of the main components of lignocellulosic biomass has been investigated [34–42]. Imidazolium based ILs (with different radicals joined to the central ring and combined with simple inorganic and more complex organic anions) have been deeply investigated for the selective dissolution of lignin, since they are not good solvents for cellulose or hemicellulose [43–45]. The ILs based on 1,3-dialkyl-imidazolium have been object of most research works. However, the limited stability of these ILs in alkaline and oxidant media must be taken into account because posterior treatment of lignin can take place under these conditions [12]. Therefore, alternative ILs non-based on imidazolium have been tested for lignin processing, paying special attention to ILs based on ammonium, phosphonium, pyridinium, and pyrrolidinium [46–49]. Nevertheless, the high economic costs derived from the employment of this type of IL remains the main drawback for real-scale implementation in the biorefinery processes [50].

Supported liquid membranes (SLMs) consist of porous supports that have been impregnated with a specific solvent to get it imbedded in the pores. The solvent is kept there by capillary forces and forms a three-phase system, since it separates the feed and stripping phases [51,52]. When this solvent is an IL, a supported ionic liquid membrane (SILM) is obtained (Figure 2) [53]. SILMs require the existence of three simultaneous processes to be applied for effective separation of solutes: the extraction from the feed solution to the SILM, the diffusion through the SILM and the re-extraction from the SILM to the stripping solution. SILMs present some advantages over SLMs, mainly because of their improved stability, since the use of ILs reduces the solvent losses from the support by evaporation or dispersion in the feed and stripping phases [54]. Moreover, ILs can provide very high specificity for the solutes to be separated and the small amount of IL required in a SILM can reduce the economic costs significantly.

Although scientific information about the use of membranes and ILs for lignocellulosic biomass fractionation and further processing is abundant, the integration of both tools as SILMs has not been deeply investigated. SILMs have been successfully applied for extraction of minor components that appear during vegetal biomass fractionation (for example, lipophilic compounds linked to resin, such as fatty acids or sterols) for analytical purposes [55]. The potential of these systems for extraction and purification of lignin must be studied, since SILMs can be preferred over other technologies for extraction and purification of lignin. Since the solute extraction from the feed phase and the re-extraction to the stripping phase occur in a unique stage, very simple designs are possible, avoiding complex configurations or high energy requirements (separation can be carried out without heat or pressure application). The employment of highly porous materials to support the SILMs provides a very high interfacial area for mass transfer, which allows very compact equipment. Moreover, the coupling of the extraction and stripping results in mass transport without limitations due to the

solubility limits [56]. The small amount of IL required to implement a SILM allows the selection of non-traditional ILs, which can offer better permeability and specificity for lignin without compromising the chemical structure and physicochemical properties of lignin or interfere in the characteristics of the rest of the lignocellulosic components. Lastly, the most relevant disadvantage of the use of ILs (their high economic costs) is minimized when SILMs are implemented, since the total volume of ILs required is greatly reduced [51].

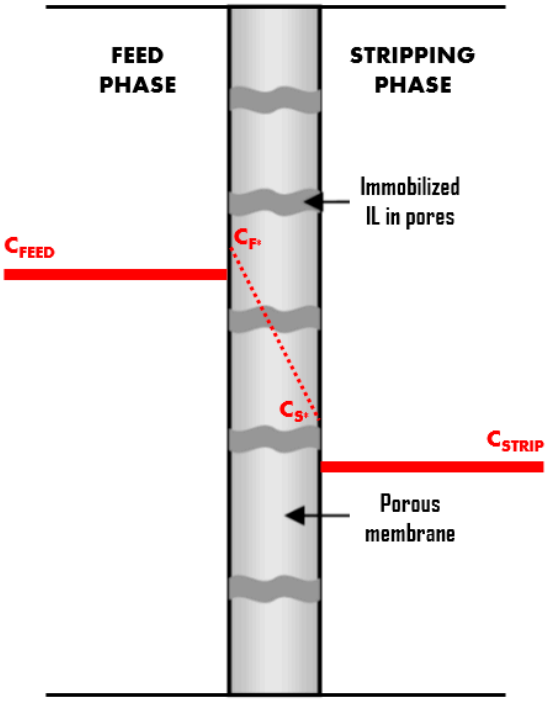

Figure 2. Schematic representation of transport through a SILM (Supported Ionic Liquid Membrane).

A previous work began the analysis of the application of SILMs for lignin separation, but the preliminary results revealed that the selective transport of lignin was not easily obtained [57]. The main objective of this work was a complete study of the potentiality of different SILMs for fractionation and separation of lignocellulosic biomass components, with special attention to lignin extraction and purification. The flow of two lignin types (Kraft lignin and lignosulphonates) from the feed compartment to the stripping one was characterized and compared with the flow of monosaccharides (glucose and xylose were selected because cellulose is made with repeated glucose units and xylose is the main sugar monomer in the structure of hemicellulose) to determine their potential for selective transport of the developed SILMs.

2. Experimental

2.1. Chemicals and Materials

Nine different ILs were selected to prepare SILMs (Figure 3). Six imidazolium-based ILs ([BMIM]$MeSO_4$, [BMIM][DBP], [BMIM][OTf] and [HMIM][OTf] from Iolitec, and [EMIM]$EtSO_4$ and [EMIM]Ac from Sigma-Aldrich, Munich, Germany), two phosphonium-based ILs (CYPHOS 101 and CYPHOS 108 from Cytec, Woodland Park, NJ, USA) and a mixture of quaternary ammonium salts (Aliquat 336 from Sigma-Aldrich, Munich, Germany) were used as supplied. Kraft lignin (low sulfonate content), D-(+)-xylose (>99%) and D-(+)-glucose (>99.5%) were provided by Sigma-Aldrich, Munich, Germany, while sodium lignosulphonate was purchased from TCI Chemicals, Tokyo, Japan. The employed water was obtained by an Elix purification system (Millipore, Darmstadt, Germany).

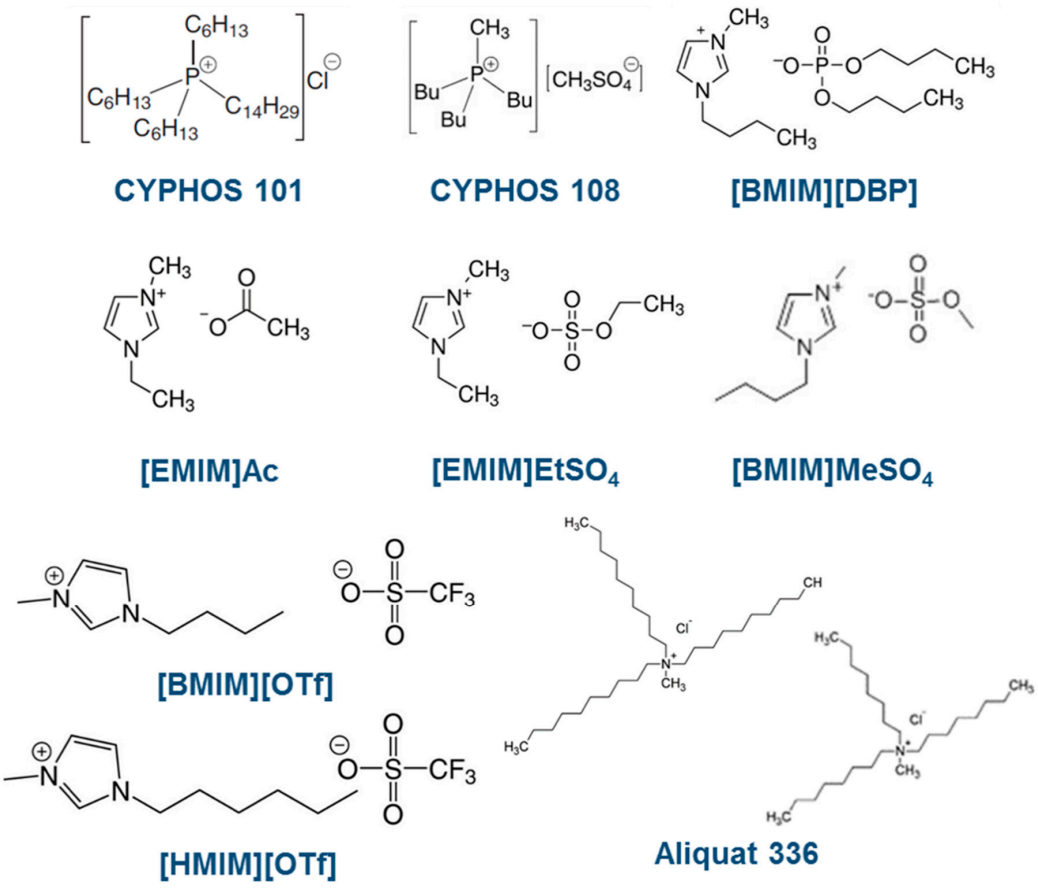

Figure 3. Structure of the selected ILs (Ionic Liquids).

As membrane supports, membrane disc filters were employed. Five different polymeric materials were tested: PP (polypropylene) and PTFE (polytetrafluoroethylene) from Filter-Lab, Barcelona, Spain, PCTE (polycarbonate) from Sterlitech, Kent, WA, USA, PVDF (hydrophobic polyvinylidene fluoride), and HPVDF (hydrophilic polyvinylidene fluoride) from Millipore, Darmstadt, Germany. All the membranes had the same diameter (47 mm) and pore diameter (0.45 μm), except PCTE (0.40 μm).

2.2. SILMs Preparation

The SILMs were prepared using the different polymeric membranes and ILs. Firstly, the corresponding membrane and IL were introduced in a vacuum oven (<35 mbar and 70 °C) within separate Petri dishes to remove the humidity, gases, and any other traces of volatile compounds. Later, the membrane was soaked in the IL, keeping the vacuum for 24 h to promote a proper impregnation by removal of air from the membrane pores. Finally, the liquid excess over the membrane surface was removed by allowing dripping overnight. This way, the SILM was ready to be employed.

2.3. Installation and Analytical Procedures

The experimental tests were carried out in a membrane cell designed for this specific purpose (Figure 4). The glass cell was composed of two identical compartments (volume lower than 150 mL each compartment), one for the feed solution and the other for the stripping one, which were separated by the SILM. The feed and stripping solutions were poured into the cell at the same time and the compartments were closed without inlet or outlet streams in the system. Samples were taken at regular time intervals from both compartments. All the experiments were carried out at room temperature. It was decided to stop the experiments after the capture of enough samples to characterize the transport.

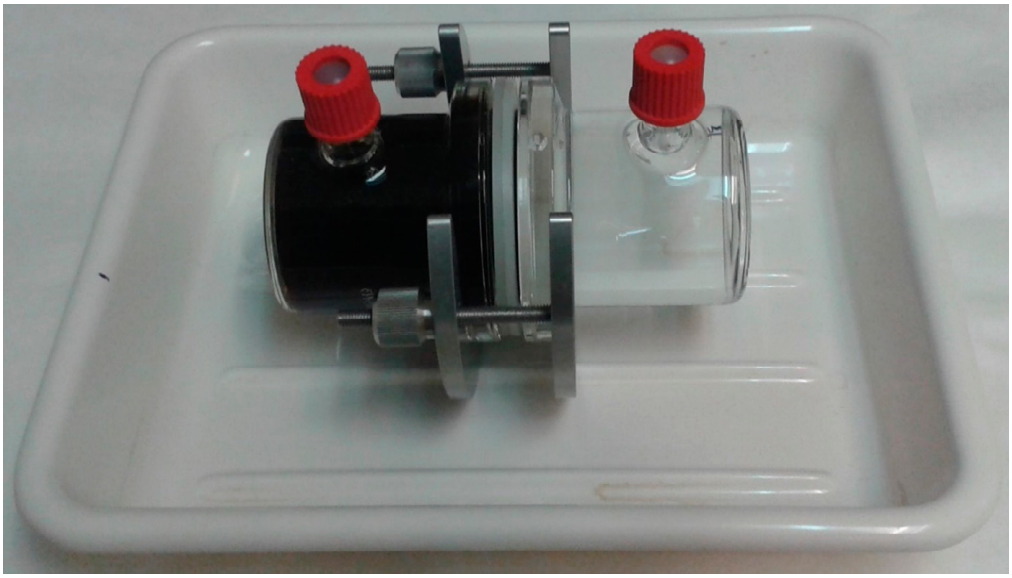

Figure 4. Image of the experimental cell selected for testing SILMs.

Kraft lignin, lignosulphonate, glucose and xylose concentrations were determined by a ultraviolet–visible (UV-VIS) spectrophotometer DR 5000 (Hach, Düsseldorf, Germany), using a wavelength of 280 nm for Kraft lignin and lignosulphonate [58,59] and of 575 nm for monosaccharides, according to the dinitrosalicylic acid method for determination of reducing sugars [60,61]. The calibration curves for the different solutes are compiled in Figure 5.

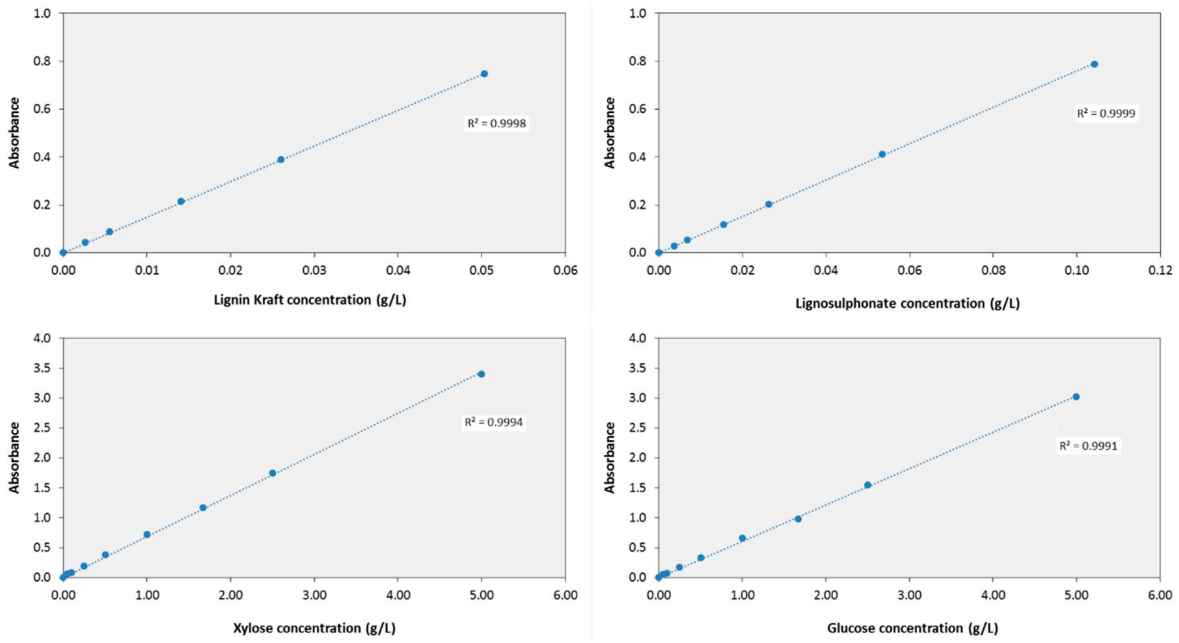

Figure 5. Calibration curves for the determination by ultraviolet–visible (UV-VIS) spectrophotometry of the concentration of the different tested solutes.

The calibration curves showed good linearity in the defined intervals (until 0.05 g/L for Kraft lignin, 0.10 g/L for lignosulphonate and 5.00 g/L for monosaccharides). From the obtained lines, the corresponding absorptivity coefficients a_λ were calculated according to the Beer–Lambert law:

$$A = a_\lambda \cdot b \cdot C \tag{1}$$

where A is the absorbance, b is the length of the path and C the solute concentration. The obtained absorptivity coefficients are compiled in Table 1.

Table 1. The absorptivity coefficients for determination by UV-VIS spectrophotometry of the concentration of the different tested solutes.

	Absorptivity Coefficients (L/g·cm)	
	a_{280}	a_{575}
Kraft lignin	14.706	-
Lignosulphonate	7.604	-
Xylose	-	0.687
Glucose	-	0.608

2.4. Membrane Transport Characterization

The previously published paper with preliminary results presented a transport model for the selective transport of solutes through the prepared SILMs [57]. However, the preliminary results revealed that the transport through the SILMs was not selective. Therefore, in this section the previously prepared model for the selective transport is summarized and the adaptations required to consider non-selective transport are added.

The amount of a solute that passes by selective transport through a SILM per unit of time and surface is called flux J and it is proportional to the gradient of concentration C between both solutions:

$$J = k \cdot \Delta C \tag{2}$$

where k is the proportionality constant that can be defined as the permeability. To model the evolution of the concentration of the solute in the feed compartment C_F, a mass balance to the feed compartment can be applied:

$$V \cdot \frac{dC_F}{dt} = -k \cdot \Delta C \cdot A_M \tag{3}$$

where V is the volume of the feed solution and A_M the active surface of the SILM. The equation can be reorder and modified considering the gradient between the feed (F) and stripping (S) compartments, and the total mass balance with C_0 as initial feed concentration

$$\Delta C = C_F - C_S \tag{4}$$

$$C_0 = C_F + C_S \tag{5}$$

$$\frac{dC_F}{2C_F - C_0} = -\frac{k \cdot A_M \cdot dt}{V} \tag{6}$$

All the constant can be grouped into a unique constant K, called effective mass transfer constant:

$$\frac{dC_F}{C_F - \frac{C_0}{2}} = -\frac{2 \cdot k \cdot A_M \cdot dt}{V} = -K \cdot dt \tag{7}$$

Integration can be applied and the evolution of the concentration in the feed compartment C_F can be assessed:

$$C_F = \frac{C_0}{2} \cdot \left(1 + e^{-K \cdot t}\right) \quad (8)$$

In a totally equivalent way, the evolution of the concentration in the stripping compartment C_S can be obtained:

$$C_S = \frac{C_0}{2} \cdot \left(1 - e^{-K \cdot t}\right) \quad (9)$$

For the case of non-selective transport, the corresponding mass balance can be formulated, just by replacement of the proportionality constant k by the permeate flux F_P:

$$V \cdot \frac{dC_F}{dt} = -F_P \cdot \Delta C \cdot A_M \quad (10)$$

This way, the evolution of the concentrations in both compartments can be derived, defining a new effective mass transfer constant K_P:

$$C_F = \frac{C_0}{2} \cdot \left(1 + e^{-K_P \cdot t}\right) \quad (11)$$

$$C_S = \frac{C_0}{2} \cdot \left(1 - e^{-K_P \cdot t}\right) \quad (12)$$

$$K_P = \frac{2 \cdot F_P \cdot A_M}{V} \quad (13)$$

3. Results and Discussion

During the preparation of the SILMs, some experimental drawbacks were identified. For example, when lignosulphonate solutions were mixed with Aliquat 336 or CYPHOS 101, unstable systems were obtained, since sticky precipitated solids appeared (Figure 6a,b). Under these conditions, a SILM with CYPHOS 101 in PVDF support did not result in effective results for Kraft lignin transport, because of the precipitation of solids on the membrane surface (Figure 6c).

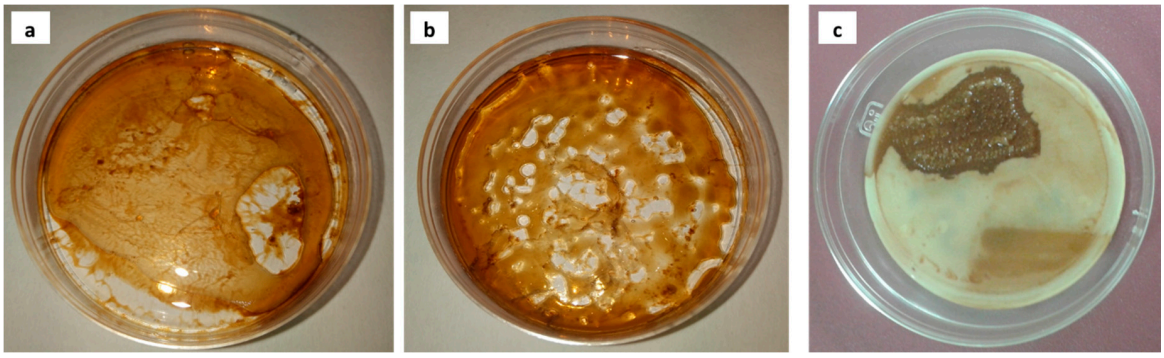

Figure 6. Identification of unstable IL and lignin systems: (**a**) 1.4 g Aliquat + 1.6 g lignosulphonate solution (40 g/L). (**b**) 1.6 g CYPHOS 108 + 1.9 g lignosulphonate solution (40 g/L). (**c**) CYPHOS 108 in PVDF support after contact with Kraft lignin solution (40 g/L).

Another identified problematic issue was the employment of [EMIM]Ac for the preparation of SILMs. After the contact between [EMIM]Ac and the PCTE support for 24 h at 70 °C in the vacuum oven, the membrane was totally dissolved in the IL (Figure 7a). Even when the temperature in the vacuum oven was reduced to 30 °C, the PCTE membrane suffered severe degradation after contact with this IL (Figure 7b). Other membranes, like PVDF or HPVDF, were highly modified (color changed)

after impregnation with [EMIM]Ac at 70 °C (Figure 7c), but a decreased value of the temperature in the vacuum oven (30 °C) resulted in stable SILMs.

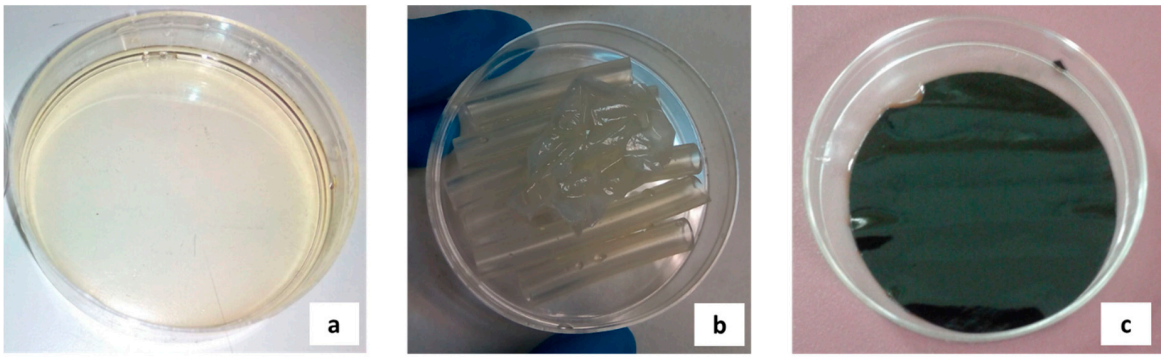

Figure 7. Identification of unstable SILMs with [EMIM]Ac: (**a**) PCTE in [EMIM]Ac (oven at 70 °C). (**b**) PCTE in [EMIM]Ac (oven at 30 °C). (**c**) HPVDF in [EMIM]Ac (oven at 70 °C).

The only virgin membrane that was permeable to Kraft lignin solution and allowed the transport of the solute from the feed to the stripping compartment was the HPVDF membrane. The evolution of the normalized concentration of Kraft lignin in the stripping compartment of the cell with respect to time is shown in Figure 8, where the transport through the virgin membrane was compared to the transport through some SILMs based on HPVDF. As can be observed in the graph, the virgin membrane showed the fastest transport, while the performance of the permeable SILMs was very similar and only minor differences could be identified among the different ILs.

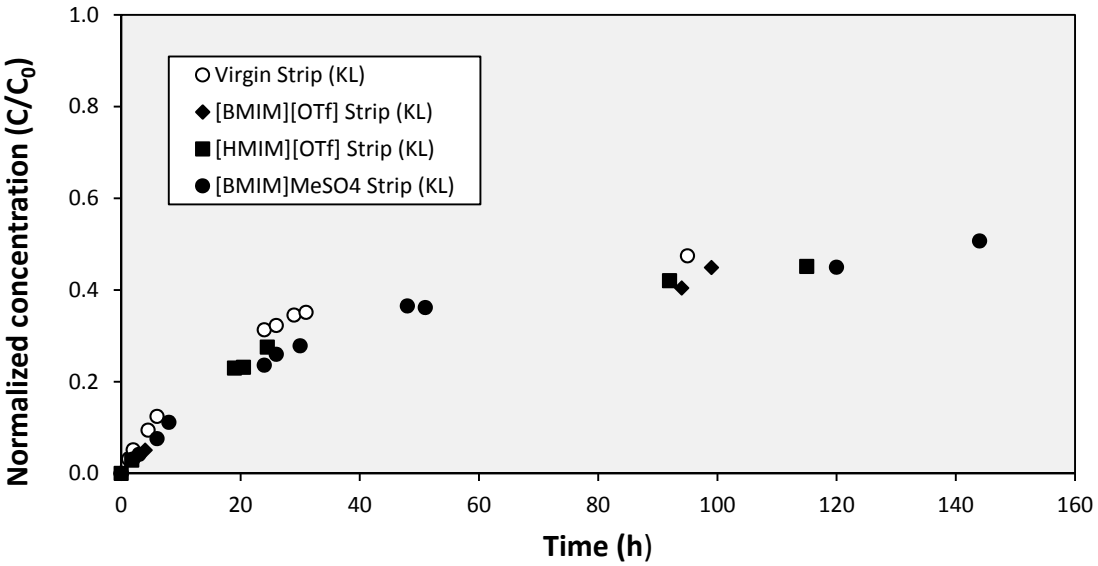

Figure 8. Evolution of the concentration of Kraft lignin in the stripping compartment with virgin HPVDF membrane and three SILMs supported in HPVDF.

Higher permeation of Kraft lignin occurred during the initial experimental phase, when the solute concentration gradient was maximum between both compartments of the cell. Then, the transport was slowed down due to reduced gradient for concentrations getting closer to the equilibrium. These experimental results fitted satisfactorily with the proposed model for non-selective transport through permeable membranes. The corresponding equations were employed for direct assessment of the effective mass transfer constants K_P (values compiled in Table 2). The R^2 values of the fitting of the

experimental results ranged from 0.936 to 0.982. As expected from the experimental results in Figure 8, the maximal K_P value corresponded to the virgin HPVDF membrane (0.0334 h^{-1}), with lower values for the HPVDF-based SILMs. Taking into account the effective membrane area in the cell (14.6 cm^2) and the volume of each cell compartment (120 mL), the corresponding permeate flux F_P were calculated from the effective mass transfer constants K_P (Table 2).

Table 2. Values of effective mass transfer constants K_P, permeate fluxes F_P, and resistances (attributable to the membrane support and the IL) for virgin HPVDF membranes and SILMs based on these membranes (viscosity and density values of the ILs are included).

	K_P (h^{-1})	F_P (m/h)	R_{MEMB} (h/m)	R_{IL} (h/m)	Viscosity [1] (mPa·s)	Density (g/cm^3)
Virgin HPVDF	0.0334	1.37×10^{-3}	729	-	-	-
HPVDF + [EMIM]$EtSO_4$	0.0263	1.08×10^{-3}	-	197	122	1.20 (80 °C)
HPVDF +[BMIM]$MeSO_4$	0.0216	0.89×10^{-3}	-	398	214	1.17 (80 °C)
HPVDF + CYPHOS 108	0.0238	0.98×10^{-3}	-	294	409	1.07 (25 °C)
HPVDF + [EMIM]Ac	0.0248	1.02×10^{-3}	-	253	93	1.07 (80 °C)
HPVDF + [BMIM][DBP]	0.0141	0.58×10^{-3}	-	997	1539	1.04 (40 °C)
HPVDF + [HMIM][OTf]	0.0157	0.65×10^{-3}	-	821	135	1.24 (29 °C)
HPVDF + [BMIM][OTf]	0.0225	0.92×10^{-3}	-	353	75	1.30 (25 °C)

[1] Measured at room temperature.

The maximal permeate flux of the virgin membrane can be directly justified taking into consideration the resistances in the series model, since the ILs supported in the membranes provide an additional resistance to the permeate transport:

$$F_P = \frac{1}{R_{TOT}} = \frac{1}{R_{MEMB} + R_{IL}} \quad (14)$$

The value of the membrane resistance R_{MEMB} was calculated from the F_P value of the virgin membrane and the resistance values attributable to the ILs were derived from the corresponding F_P values once R_{MEMB} was known. According to the figures in Table 2, the R_{IL} values were lower than the R_{MEMB} value for all the SILMs but the ones with [BMIM][DBP] and [HMIM][OTf]. The high resistance exhibited by [BMIM][DBP] can be directly attributed to its high viscosity, but the value corresponding to [HMIM][OTf] was not easily related to the viscosity or density of the IL because other more viscous or denser ILs showed lower resistance [62–67].

Apart from HPVDF, the rest of the virgin membranes were impermeable to water or aqueous solutions. The SILMs prepared with these impermeable membranes were initially tested with Kraft lignin and lignosulphonate solutions. The results obtained with some of these SILMs are graphed in Figure 9, where the evolution of the solute concentration in both compartments is presented. The differences among the experimental data for SILMs with different ILs and solutes were not obvious and very similar results were obtained for all the SILMs that exhibited solute transport. When additional experiments were carried out with monosaccharides (glucose and xylose) as solutes, the performance of the tested SILMs was comparable and the evolution of the monosaccharides concentration in the cell compartments followed a similar trend to the identified one for Kraft lignin or lignosulphonates (Figure 10). A further analysis of the experimental results shown in Figures 8–10 suggested non-selective transport through the SILMs, as the different investigated membranes, ILs or solutes had not relevant influence on the performance of the SILMs. For example, the performance of the SILMs based on impermeable membranes could be compared to the SILMs based on permeable HPVDF.

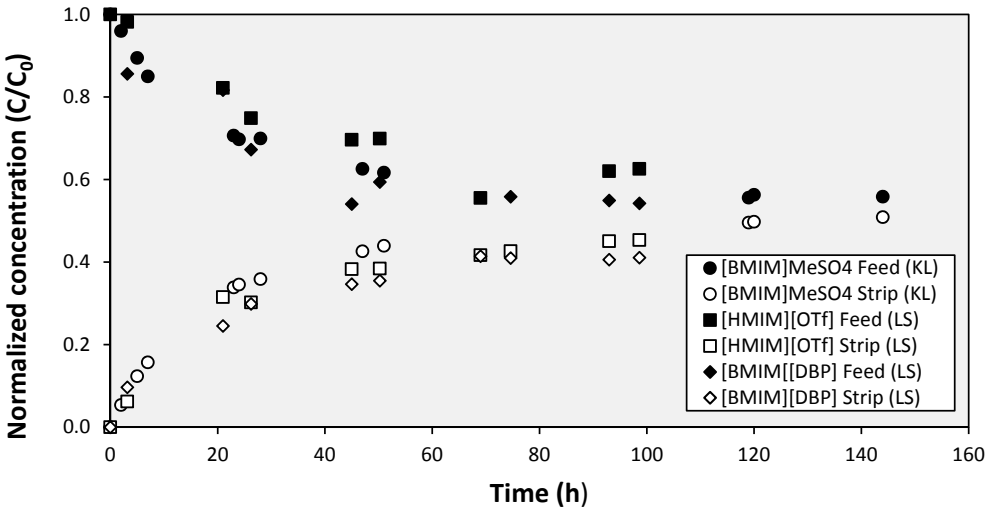

Figure 9. Evolution of the concentration of Kraft lignin (KL) or lignosulphonate (LS) in the feed and stripping compartments with three different SILMs supported in PCTE.

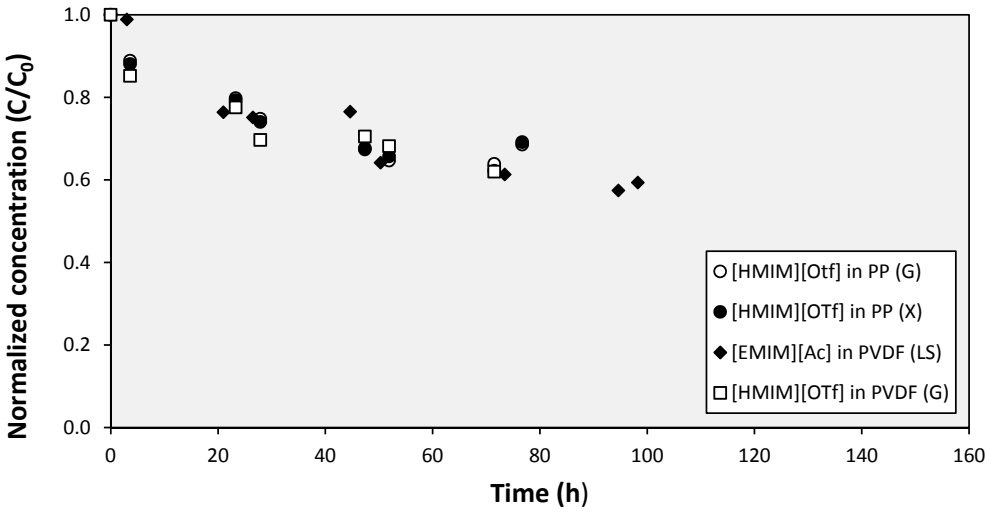

Figure 10. Evolution of the concentration of lignosulphonate (LS), glucose (G), or xylose (X) in the feed compartment with three different SILMs.

The lack of selectivity of the studied SILMs was previously reported during the preliminary works of this research group [57]. Those results demonstrated that the performance of the freshly prepared SILMs was totally similar to SILMs used repeatedly in consecutive cycles, even when the IL had been apparently lost from the membrane support. The mass loss of the SILMs once the first cycle was finished corresponded to the amount of IL previously immobilized in the membrane. Scanning electron microscope (SEM) images confirmed this fact, since the appearance of the membrane before the second cycle was much more similar to the virgin membrane than the SILM before the first cycle (Figure 11). Therefore, the transport through the SILMs seemed to be more closely related to the modification of the membrane supports than the presence of ILs in the membranes. Further experiments were carried out to understand the transport through the SILMs and tests to analyze the permeability of the SILMs to water and aqueous solutions were proposed. While the feed compartment was filled with water or an aqueous solution of Kraft lignin, the stripping compartment remained empty. Surprisingly, nearly all the tested SILMs that exhibited solute transport were identified as permeable and the only SILM that maintained its impermeability was that one based on [BMIM][DBP] supported in PTFE (Figure 12).

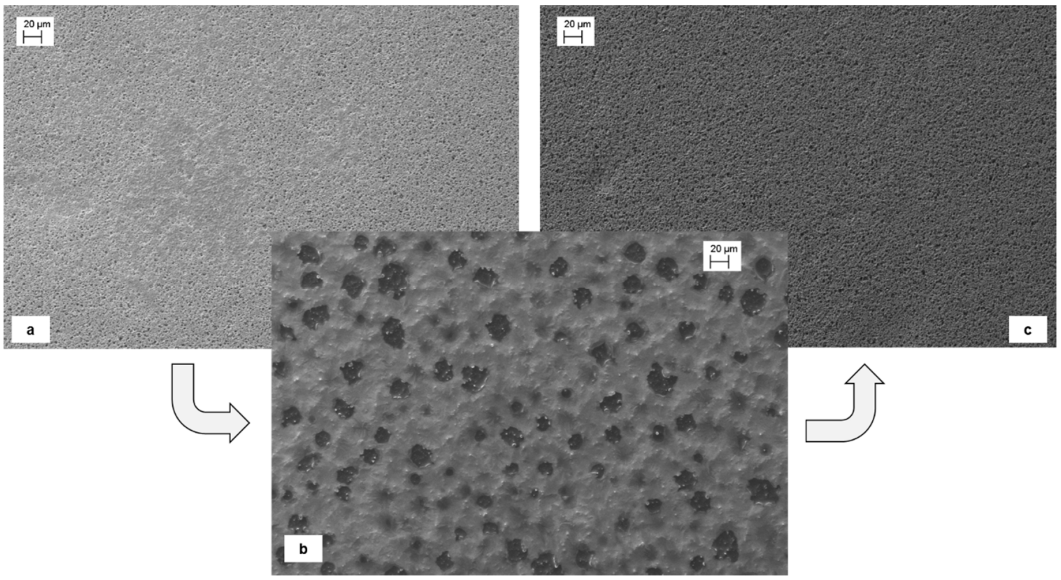

Figure 11. Scanning electron microscope (SEM) microphotographs of virgin PVDF membrane (**a**), SILM with CYPHOS 108 in PVDF before the transport test (**b**) and SILM with CYPHOS 108 in PVDF after the transport test (**c**).

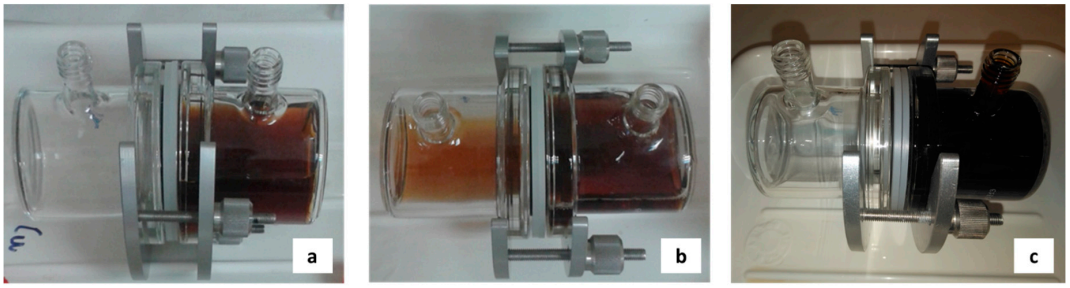

Figure 12. Images of the permeability tests of virgin PVDF membrane (**a**), SILM with CYPHOS 108 in PVDF (**b**), and SILM with [BMIM][DBP] in PTFE (**c**).

As a summary, Table 3 compiles all the calculated K_P values of the tested SILMs. Moreover, the same table identifies the SILMs that were not tested because of the technical drawbacks during their preparation and the SILMS that did not show any solute transport. The reported K_P values ranged between 0.0139 and 0.0284 h^{-1} for [BMIM][DBP] in PP and [BMIM]$MeSO_4$ in PCTE, respectively. These figures fell in the range of the SILMS prepared with HPVDF (0.0141–0.0263 h^{-1}). This concordance once again confirmed the common transport mechanisms between both types of SILMs: convective transport of the solute as consequence of the permeation of the solutions.

The SILM with [BMIM][DBP] supported in PTFE membrane, which was the only one that showed impermeability to the tested solutions, was the only case that exhibited selective solute transport. As can be observed in Figure 13, the evolution of the concentration in the stripping compartment was very different for the two graphed solutes: the transport of glucose is much faster than the transport of lignosulphonate. While in the case of glucose, 70 h was time enough to achieve a concentration that could be considered an equilibrium situation; after 100 h the normalized concentration of lignosulphonate in the stripping compartment was still below 0.38.

Table 3. Summary table with the values of effective mass transfer constants K_P of the different tested SILMs.

Membrane Support	K_P (h^{-1})								
	CYPHOS 101	**CYPHOS 108**	**ALIQUAT**	**[BMIM]$MeSO_4$**	**[BMIM][DBP]**	**[BMIM][OTf]**	**[HMIM][OTf]**	**[EMIM]$EtSO_4$**	**[EMIM]Ac**
HPVDF	No tested	0.0238	No tested	0.0216	0.0141	0.0225	0.0157	0.0263	0.0248
PVDF	No tested	0.0254	No tested	0.0238	0.0247	0.0221	0.0171	0.0237	0.0186
PCTE	No tested	No tested	No tested	0.0284	0.0225	No tested	0.0227	No tested	No tested
PP	No tested	0.0248	No tested	No transport	0.0139	0.0179	0.0182	No transport	No transport
PTFE	No tested	No transport	No tested	No transport	Selective transport	No transport	No transport	No transport	No transport

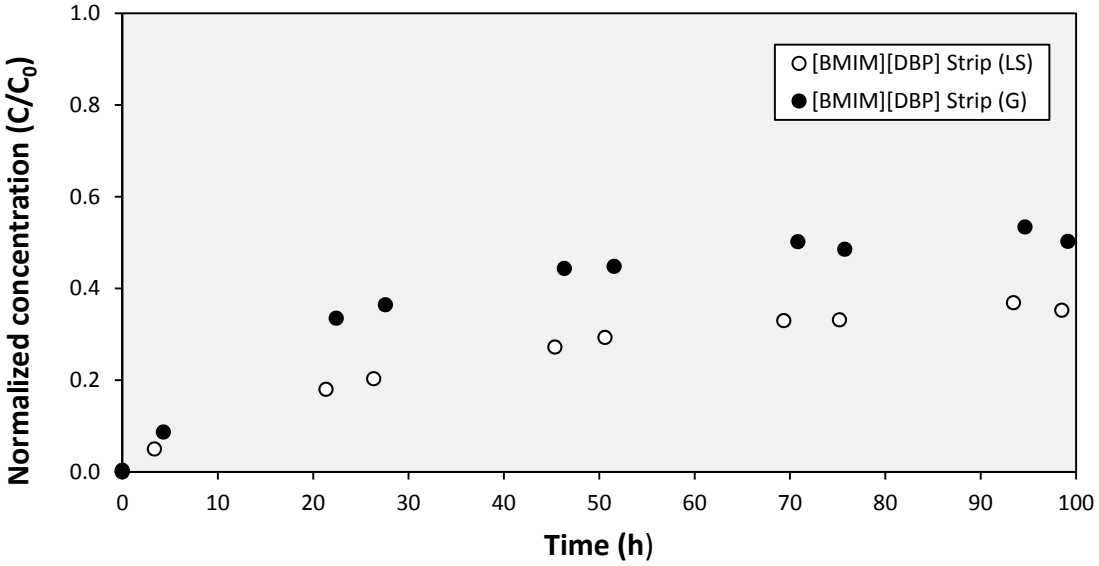

Figure 13. Evolution of the concentration of lignosulphonate (LS), glucose (G) in the stripping compartment with SILM with [BMIM][DBP] in PTFE.

When Kraft lignin and xylose were selected as solutes, the results were equivalent. The transport of xylose was much faster, with very similar results to glucose, and the results of Kraft lignin and lignosulphonates were comparable. The corresponding effective mass transfer constants were calculated (Table 4). These values revealed that glucose was the most easily transported solute, followed by xylose. The lignin compounds showed lower values: 0.67×10^{-3} m/h for lignosulphonate and 0.71×10^{-3} m/h for Kraft lignin. Therefore, the transport of monosaccharides was favored against lignin compounds. Further work will be carried out in order to improve the understanding of the mechanisms of the selective transport through the SILM and its stability. Furthermore, the design of effective separation processes based on this SILM will be investigated.

Table 4. Values of effective mass transfer constants K, and permeabilities k of the SILMs based on [BMIM][DBP] supported in PTFE membranes.

	K (h^{-1})	k (m/h)
Kraft lignin (KL)	0.0172	0.71×10^{-3}
Lignosulphonate (LS)	0.0162	0.67×10^{-3}
Glucose (G)	0.0453	1.86×10^{-3}
Xylose (X)	0.0429	1.76×10^{-3}

4. Conclusions

This study investigated the potential of SILMs for selective transport of two different types of technical lignins (Kraft lignin and lignosulphonate) and monosaccharides (xylose and glucose) in an aqueous solution. The SILMs obtained by the combination of five different membrane supports and nine ILs were tested. Some ILs (CYPHOS 101 and Aliquat 336) were not useful, since they resulted in unstable SILMs because of precipitation problems. [EMIM]Ac was another problematic IL as it degraded some of the membrane supports. Although the virgin hydrophobic membranes did not allow the permeation of the aqueous solutions, most membranes became permeable after the impregnation with the ILs. Therefore, the solutes were able to cross these SILMs by non-selective transport. However, the SILM based on [BMIM][DBP] as IL and PTFE as membrane support maintained its hydrophobicity and allowed selective transport of the tested solutes. The effective mass transfer constants of the solutes were determined according to the proposed transport model: lignosulphonate was the

least easily transported solute (0.67×10^{-3} m/h), while glucose was the most easily transported one (1.86×10^{-3} m/h). Nevertheless, the stability of this identified selective SILM and its applicability to separation processes must be investigated more deeply and further work will be carried out.

Author Contributions: R.A. conceived and designed the experiments; J.R., S.L. and A.A. performed the experiments; R.A., J.R., S.L. and A.A. analyzed the data; A.G. and A.I. supervised the investigation; R.A. prepared the original draft of the manuscript and all authors revised the several versions of the manuscript.

Funding: This research has been financially supported by the Spanish Ministry of Economy and Competitiveness (MINECO) through CTQ2014-56820-JIN Project, co-financed by FEDER funds from European Union.

Conflicts of Interest: The authors declare no conflict of interest.

References

1. Bjärstig, T.; Sténs, A. Social Values of Forests and Production of New Goods and Services: The Views of Swedish Family Forest Owners. *Small-Scale For.* **2018**, *17*, 125–146. [CrossRef]
2. Hamaguchi, M.; Kautto, J.; Vakkilainen, E. Effects of hemicellulose extraction on the kraft pulp mill operation and energy use: Review and case study with lignin removal. *Chem. Eng. Res. Des.* **2013**, *91*, 1284–1291. [CrossRef]
3. Abejón, R. A Bibliometric Study of Scientific Publications regarding Hemicellulose Valorization during the 2000–2016 Period: Identification of Alternatives and Hot Topics. *ChemEngineering* **2018**, *2*, 7. [CrossRef]
4. Abejón, R.; Pérez-Acebo, H.; Clavijo, L. Alternatives for Chemical and Biochemical Lignin Valorization: Hot Topics from a Bibliometric Analysis of the Research Published During the 2000–2016 Period. *Processes* **2018**, *6*, 98. [CrossRef]
5. Li, T.; Takkellapati, S. The current and emerging sources of technical lignins and their applications. *Biofuels Bioprod. Biorefin.* **2018**, 1–32. [CrossRef]
6. Lee, H.S.; Jae, J.; Ha, J.M.; Suh, D.J. Hydro- and solvothermolysis of kraft lignin for maximizing production of monomeric aromatic chemicals. *Bioresour. Technol.* **2016**, *203*, 142–149. [CrossRef] [PubMed]
7. Ceapraz, I.L.; Kotbi, G.; Sauvee, L. The territorial biorefinery as a new business model. *Bio-Based Appl. Econ.* **2016**, *5*, 47–62. [CrossRef]
8. De Bhowmick, G.; Sarmah, A.K.; Sen, R. Lignocellulosic biorefinery as a model for sustainable development of biofuels and value added products. *Bioresour. Technol.* **2018**, *247*, 1144–1154. [CrossRef] [PubMed]
9. Barcelos, C.A.; Maeda, R.N.; Betancur, G.J.V.; Pereira, N. The essentialness of delignification on enzymatic hydrolysis of sugar cane bagasse cellulignin for second generation ethanol production. *Waste Biomass Valorization* **2013**, *4*, 341–346. [CrossRef]
10. Pihlajaniemi, V.; Sipponen, M.H.; Pastinen, O.; Nyyssölä, A.; Laakso, S. The effect of direct and counter-current flow-through delignification on enzymatic hydrolysis of wheat straw, and flow limits due to compressibility. *Biotechnol. Bioeng.* **2016**, *113*, 2605–2613. [CrossRef] [PubMed]
11. Ragauskas, A.J.; Beckham, G.T.; Biddy, M.J.; Chandra, R.; Chen, F.; Davis, M.F.; Davison, B.H.; Dixon, R.A.; Gilna, P.; Keller, M.; et al. Lignin valorization: Improving lignin processing in the biorefinery. *Science* **2014**, *344*. [CrossRef] [PubMed]
12. Chatel, G.; Rogers, R.D. Review: Oxidation of lignin using ionic liquids-an innovative strategy to produce renewable chemicals. *ACS Sustain. Chem. Eng.* **2014**, *2*, 322–339. [CrossRef]
13. Davis, K.M.; Rover, M.; Brown, R.C.; Bai, X.; Wen, Z.; Jarboe, L.R. Recovery and utilization of lignin monomers as part of the biorefinery approach. *Energies* **2016**, *9*, 808. [CrossRef]
14. Beckham, G.T.; Johnson, C.W.; Karp, E.M.; Salvachúa, D.; Vardon, D.R. Opportunities and challenges in biological lignin valorization. *Curr. Opin. Biotechnol.* **2016**, *42*, 40–53. [CrossRef] [PubMed]
15. Rinaldi, R.; Jastrzebski, R.; Clough, M.T.; Ralph, J.; Kennema, M.; Bruijnincx, P.C.A.; Weckhuysen, B.M. Paving the Way for Lignin Valorisation: Recent Advances in Bioengineering, Biorefining and Catalysis. *Angew. Chem. Int. Ed.* **2016**, *55*, 8164–8215. [CrossRef] [PubMed]
16. Wang, W.; Zhang, C.; Sun, X.; Su, S.; Li, Q.; Linhardt, R.J. Efficient, environmentally-friendly and specific valorization of lignin: Promising role of non-radical lignolytic enzymes. *World J. Microbiol. Biotechnol.* **2017**, *33*, 1–14. [CrossRef] [PubMed]

17. Fan, M.H.; Deng, S.M.; Wang, T.J.; Li, Q.X. Production of BTX through catalytic depolymerization of lignin. *Chin. J. Chem. Phys.* **2014**, *27*, 221–226. [CrossRef]
18. Elfadly, A.M.; Zeid, I.F.; Yehia, F.Z.; Abouelela, M.M.; Rabie, A.M. Production of aromatic hydrocarbons from catalytic pyrolysis of lignin over acid-activated bentonite clay. *Fuel Process. Technol.* **2017**, *163*, 1–7. [CrossRef]
19. Holladay, J.E.; White, J.F.; Bozell, J.J.; Johnson, D. *Top Value-Added Chemicals from Biomass Volume II—Results of Screening for Potential Candidates from Biorefinery Lignin*; DOE Scientific and Technical Information; US Department of Energy: Oak Ridge, TN, USA, 2007; ISBN PNNL-16983.
20. Abels, C.; Carstensen, F.; Wessling, M. Membrane processes in biorefinery applications. *J. Memb. Sci.* **2013**, *444*, 285–317. [CrossRef]
21. Dafinov, A.; Font, J.; Garcia-Valls, R. Processing of black liquors by UF/NF ceramic membranes. *Desalination* **2005**, *173*, 83–90. [CrossRef]
22. Bhattacharya, P.K.; Todi, R.K.; Tiwari, M.; Bhattacharjee, C.; Bhattacharjee, S.; Datta, S. Studies on ultrafiltration of spent sulfite liquor using various membranes for the recovery of lignosulphonates. *Desalination* **2005**, *174*, 287–297. [CrossRef]
23. Moniz, P.; Serralheiro, C.; Matos, C.T.; Boeriu, C.G.; Frissen, A.E.; Duarte, L.C.; Roseiro, L.B.; Pereira, H.; Carvalheiro, F. Membrane separation and characterisation of lignin and its derived products obtained by a mild ethanol organosolv treatment of rice straw. *Process Biochem.* **2018**, *65*, 136–145. [CrossRef]
24. Mota, I.F.; Pinto, P.R.; Ribeiro, A.M.; Loureiro, J.M.; Rodrigues, A.E. Downstream processing of an oxidized industrial kraft liquor by membrane fractionation for vanillin and syringaldehyde recovery. *Sep. Purif. Technol.* **2018**, *197*, 360–371. [CrossRef]
25. Servaes, K.; Varhimo, A.; Dubreuil, M.; Bulut, M.; Vandezande, P.; Siika-aho, M.; Sirviö, J.; Kruus, K.; Porto-Carrero, W.; Bongers, B. Purification and concentration of lignin from the spent liquor of the alkaline oxidation of woody biomass through membrane separation technology. *Ind. Crops Prod.* **2017**, *106*, 86–96. [CrossRef]
26. Weinwurm, F.; Drljo, A.; Waldmüller, W.; Fiala, B.; Niedermayer, J.; Friedl, A. Lignin concentration and fractionation from ethanol organosolv liquors by ultra- and nanofiltration. *J. Clean. Prod.* **2016**, *136*, 62–71. [CrossRef]
27. Jönsson, A.S.; Nordin, A.K.; Wallberg, O. Concentration and purification of lignin in hardwood kraft pulping liquor by ultrafiltration and nanofiltration. *Chem. Eng. Res. Des.* **2008**, *86*, 1271–1280. [CrossRef]
28. Toledano, A.; García, A.; Mondragon, I.; Labidi, J. Lignin separation and fractionation by ultrafiltration. *Sep. Purif. Technol.* **2010**, *71*, 38–43. [CrossRef]
29. Sevastyanova, O.; Helander, M.; Chowdhury, S.; Lange, H.; Wedin, H.; Zhang, L.; Ek, M.; Kadla, J.F.; Crestini, C.; Lindström, M.E. Tailoring the molecular and thermo-mechanical properties of kraft lignin by ultrafiltration. *J. Appl. Polym. Sci.* **2014**, *131*, 9505–9515. [CrossRef]
30. Žabková, M.; da Silva, E.A.B.; Rodrigues, A.E. Recovery of vanillin from lignin/vanillin mixture by using tubular ceramic ultrafiltration membranes. *J. Memb. Sci.* **2007**, *301*, 221–237. [CrossRef]
31. Dubreuil, M.F.S.; Servaes, K.; Ormerod, D.; Van Houtven, D.; Porto-Carrero, W.; Vandezande, P.; Vanermen, G.; Buekenhoudt, A. Selective membrane separation technology for biomass valorization towards bio-aromatics. *Sep. Purif. Technol.* **2017**, *178*, 56–65. [CrossRef]
32. Werhan, H.; Farshori, A.; von Rohr, P.R. Separation of lignin oxidation products by organic solvent nanofiltration. *J. Memb. Sci.* **2012**, *423–424*, 404–412. [CrossRef]
33. Mai, N.L.; Koo, Y.M. Computer-Aided Design of Ionic Liquids for High Cellulose Dissolution. *ACS Sustain. Chem. Eng.* **2016**, *4*, 541–547. [CrossRef]
34. Hossain, M.M.; Aldous, L. Ionic liquids for lignin processing: Dissolution, isolation, and conversion. *Aust. J. Chem.* **2012**, *65*, 1465–1477. [CrossRef]
35. Isik, M.; Sardon, H.; Mecerreyes, D. Ionic liquids and cellulose: Dissolution, chemical modification and preparation of new cellulosic materials. *Int. J. Mol. Sci.* **2014**, *15*, 11922–11940. [CrossRef] [PubMed]
36. Zhao, D.; Li, H.; Zhang, J.; Fu, L.; Liu, M.; Fu, J.; Ren, P. Dissolution of cellulose in phosphate-based ionic liquids. *Carbohydr. Polym.* **2012**, *87*, 1490–1494. [CrossRef]
37. Lan, W.; Liu, C.F.; Yue, F.X.; Sun, R.C.; Kennedy, J.F. Ultrasound-assisted dissolution of cellulose in ionic liquid. *Carbohydr. Polym.* **2011**, *86*, 672–677. [CrossRef]
38. Stolarska, O.; Pawlowska-Zygarowicz, A.; Soto, A.; Rodríguez, H.; Smiglak, M. Mixtures of ionic liquids as more efficient media for cellulose dissolution. *Carbohydr. Polym.* **2017**, *178*, 277–285. [CrossRef] [PubMed]

39. Liu, R.; Chen, Z.; Ren, H.; Duan, E. Synthesis and properties of non-aromatic ionic liquids and their role in cellulose dissolution. *BioResources* **2017**, *12*, 5407–5416. [CrossRef]
40. Roselli, A.; Asikainen, S.; Stepan, A.; Monshizadeh, A.; Von Weymarn, N.; Kovasin, K.; Wang, Y.; Xiong, H.; Turunen, O.; Hummel, M.; et al. Comparison of pulp species in IONCELL-P: Selective hemicellulose extraction method with ionic liquids. *Holzforschung* **2016**, *70*, 291–296. [CrossRef]
41. Heggset, E.B.; Syverud, K.; Øyaas, K. Novel pretreatment pathways for dissolution of lignocellulosic biomass based on ionic liquid and low temperature alkaline treatment. *Biomass Bioenergy* **2016**, *93*, 194–200. [CrossRef]
42. Carneiro, A.P.; Rodriguez, O.; Macedo, E.A. Dissolution and fractionation of nut shells in ionic liquids. *Bioresour. Technol.* **2017**, *227*, 188–196. [CrossRef] [PubMed]
43. Mäki-Arvela, P.; Anugwom, I.; Virtanen, P.; Sjöholm, R.; Mikkola, J.P. Dissolution of lignocellulosic materials and its constituents using ionic liquids-A review. *Ind. Crops Prod.* **2010**, *32*, 175–201. [CrossRef]
44. Lee, S.H.; Doherty, T.V.; Linhardt, R.J.; Dordick, J.S. Ionic liquid-mediated selective extraction of lignin from wood leading to enhanced enzymatic cellulose hydrolysis. *Biotechnol. Bioeng.* **2009**, *102*, 1368–1376. [CrossRef] [PubMed]
45. Tan, S.S.Y.; MacFarlane, D.R.; Upfal, J.; Edye, L.A.; Doherty, W.O.S.; Patti, A.F.; Pringle, J.M.; Scott, J.L. Extraction of lignin from lignocellulose at atmospheric pressure using alkylbenzenesulfonate ionic liquid. *Green Chem.* **2009**, *11*, 339. [CrossRef]
46. Balaji, C.; Banerjee, T.; Goud, V.V. COSMO-RS based predictions for the extraction of lignin from lignocellulosic biomass using ionic liquids: Effect of cation and anion combination. *J. Solut. Chem.* **2012**, *41*, 1610–1630. [CrossRef]
47. Hamada, Y.; Yoshida, K.; Asai, R.; Hayase, S.; Nokami, T.; Izumi, S.; Itoh, T. A possible means of realizing a sacrifice-free three component separation of lignocellulose from wood biomass using an amino acid ionic liquid. *Green Chem.* **2013**, *15*, 1863. [CrossRef]
48. Prado, R.; Erdocia, X.; Labidi, J. Lignin extraction and purification with ionic liquids. *J. Chem. Technol. Biotechnol.* **2013**, *88*, 1248–1257. [CrossRef]
49. Glas, D.; Van Doorslaer, C.; Depuydt, D.; Liebner, F.; Rosenau, T.; Binnemans, K.; De Vos, D.E. Lignin solubility in non-imidazolium ionic liquids. *J. Chem. Technol. Biotechnol.* **2015**, *90*, 1821–1826. [CrossRef]
50. Konda, N.M.; Shi, J.; Singh, S.; Blanch, H.W.; Simmons, B.A.; Klein-Marcuschamer, D. Understanding cost drivers and economic potential of two variants of ionic liquid pretreatment for cellulosic biofuel production. *Biotechnol. Biofuels* **2014**, *7*, 1–11. [CrossRef] [PubMed]
51. Parhi, P.K. Supported liquid membrane principle and its practices: A short review. *J. Chem.* **2013**, *2013*. [CrossRef]
52. Kocherginsky, N.M.; Yang, Q.; Seelam, L. Recent advances in supported liquid membrane technology. *Sep. Purif. Technol.* **2007**, *53*, 171–177. [CrossRef]
53. Abejón, R.; Pérez-Acebo, H.; Garea, A. A Bibliometric Analysis of Research on Supported Ionic Liquid Membranes during the 1995–2015 Period: Study of the Main Applications and Trending Topics. *Membranes* **2017**, *7*, 63. [CrossRef] [PubMed]
54. Lozano, L.J.; Godínez, C.; de los Ríos, A.P.; Hernández-Fernández, F.J.; Sánchez-Segado, S.; Alguacil, F.J. Recent advances in supported ionic liquid membrane technology. *J. Memb. Sci.* **2011**, *376*, 1–14. [CrossRef]
55. Kilulya, K.F.; Msagati, T.A.M.; Mamba, B.B.; Ngila, J.C.; Bush, T. Ionic liquid-liquid extraction and supported liquid membrane analysis of lipophilic wood extractives from dissolving-grade pulp. *Chromatographia* **2012**, *75*, 513–520. [CrossRef]
56. Venkateswaran, P. Di (2-ethylhexyl) phosphoric acid-coconut oil supported liquid membrane for the separation of copper ions from copper plating wastewater. *J. Environ. Sci.* **2007**, *19*, 1446–1453. [CrossRef]
57. Abejón, R.; Abejón, A.; Garea, A.; Irabien, A. Transport of lignin and other lignocellulosic components through supported ionic liquid membranes. *Chem. Eng. Trans.* **2017**, *57*, 1153–1158.
58. Alén, R.; Hartus, T. UV spectrophotometric determination of lignin from alkaline pulping liquors. *Cell. Chem. Technol.* **1987**, *618*, 613–618.
59. Lee, R.A.; Bédard, C.; Berberi, V.; Beauchet, R.; Lavoie, J.M. UV-Vis as quantification tool for solubilized lignin following a single-shot steam process. *Bioresour. Technol.* **2013**, *144*, 658–663. [CrossRef] [PubMed]
60. Miller, G.L. Use of Dinitrosalicylic Acid Reagent for Determination of Reducing Sugar. *Anal. Chem.* **1959**, *31*, 426–428. [CrossRef]

61. Oveissi, F.; Fatehi, P. Isolating lignin from spent liquor of thermomechanical pulping process via adsorption. *Environ. Technol.* **2014**, *35*, 2597–2603. [CrossRef] [PubMed]
62. Iolitec Ionic liquids: Catalogue. Available online: https://iolitec.de/index.php/en/products/ionic_liquids/catalogue (accessed on 6 June 2018).
63. Zhang, S.; Zhou, Q.; Lu, X.; Song, Y.; Wang, X. *Physicochemical Properties of Ionic Liquid Mixtures*; Springer: Dordrecht, The Netherlands, 2016; ISBN 9789401775717.
64. Palgunadi, J.; Kang, J.E.; Cheong, M.; Kim, H.; Lee, H.; Kim, H.S. Fluorine-free imidazolium-based ionic liquids with a phosphorous-containing anion as potential CO_2 absorbents. *Bull. Korean Chem. Soc.* **2009**, *30*, 1749–1754. [CrossRef]
65. Ge, M.-L.; Zhao, R.-S.; Yi, Y.-F.; Zhang, Q.; Wang, L.-S. Densities and Viscosities of 1-Butyl-3-methylimidazolium Tetrafluoroborate + H_2O Binary Mixtures at T = (303.15 to 343.15) K. *J. Chem. Eng. Data* **2008**, *53*, 2408–2411. [CrossRef]
66. Fredlake, C.P.; Crosthwaite, J.M.; Hert, D.G.; Aki, S.N.V.K.; Brennecke, J.F. Thermophysical Properties of Imidazolium-Based Ionic Liquids. *J. Chem. Eng. Data* **2004**, *49*, 954–964. [CrossRef]
67. Fraser, K.J.; MacFarlane, D.R. Phosphonium-based ionic liquids: An overview. *Aust. J. Chem.* **2009**, *62*, 309–321. [CrossRef]